Transaction B: Mechanical Engineering
Vol. 16, No. 3, pp. 212–221

Radiative Transfer in the Fine Structures of Quiescent Prominences

A. Ajabshirizadeh[1,2], A.G. Nikoghossian[2,3] and H. Ebadi[1,2,4,*]

Abstract. *In this paper, elaborating the statistical approach recently proposed by one of the present authors (A.G.N) has been elaborated for interpretation of the spatial brightness variations of solar quiescent prominences. The mean statistical characteristics of the LTE line radiation such as the mean intensity and its Relative Mean Square Deviation (RelMSD) emerging from a multi-component atmosphere with randomly varying properties are derived as the functions of the frequency within a line. The results previously obtained are extended to encompass more realistic models when fluctuations of the observed line intensities represent a combined effect of variation of different physical and geometrical parameters of the medium (internal energy sources, optical thickness, velocity field, the number of structural elements along the line of sight etc.). It is shown that the center-to-wings evolution of the RelMSD essentially depends on the mentioned features of the atmosphere, which are responsible for the spatial variations we observe. The obtained results are applied to the EUV-lines through SUMER spectrometer in frameworks of the SOHO space mission. As a rule, the observed values of RelMSD in the central frequencies of the observed lines are less than those in the wings. This points out that the observed fluctuations are mainly due to the changes in energy sources in the prominence. It is shown that the central dispersion of the RelMSD correlates with the characteristic temperature of a given line formation.*

Keywords: *Sun; Radiative transfer; Quiescent prominence; Fine structure.*

INTRODUCTION

The solar quiescent prominences are known as relatively cold and dense formations imbedded in hot and strongly magnetized plasma of transition region and corona. They are characterized by a rather complex fine structure, which offers difficulties in theoretical interpretation of the spectral line profiles and their changes we observe. However, one may expect that some information on the physical and geometrical features of a radiating medium may be gained by studying the spatial variations of the prominence surface brightness in different frequencies within spectral lines. Pursuing this aim, we assume that the intensity fluctuations observed in passing from one pixel to another are due to the random character of the geometrical and physical properties of the structural elements and the medium as a whole. Hence, when observing certain distributions of intensity over the set of pixels, we are concerned with an ensemble of various realizations of these characteristics. This stresses the need for developing a suitable theory of the line formations, which will allow for the presence of randomly varying structural pattern heterogeneities. An analytical procedure for handling the randomized problems of the radiative transfer in the line frequencies was explored by one of the present authors recently [1-4]. As a result, the effect of random variations of the optical thickness of structural elements and the power of internal energy sources on the line profiles and relative mean square deviation (RelMSD) of intensity escaping from the radiating medium were found out. Both the Local Thermodynamic (LTE) and Non-LTE cases were considered. In its general formulation the problem encounters essential difficulties in the case of Non-LTE lines because of scattering, which leads to the appearance of fluxes reflected from structural elements. It should be noted that prominences are far from the LTE state. Namely, cool lines are formed

1. *Faculty of Physics, Tabriz University, Tabriz, Iran.*
2. *Research Institue for Astronomy and Astrophysics of Maragha, Maragha, P.O. Box 55134-441, Iran.*
3. *Byurakan Astrophysical Observatory, 378433 Byurakan, Armenia.*
4. *Instititut d'Astrophysique Spatiale, Unit Mixte CNRS-Universite de Paris XI, Bat 121, 91405 Orsay, France.*
*. *Corresponding author. E-mail: h_ebadie@yahoo.com*

Received 21 January 2007; received in revised form 19 November 2007; accepted 12 April 2008

by a scattering of incident solar radiation and, thus, their source function is mainly driven by the intensity of this radiation. In the prominence corona transition region, the scattering may play a role for some ions, but this formalism in a Non-LTE case is much more complicated and will be treated in future works. Of special interest in this connection is revealing the role of fluctuations of the destruction coefficient [4,5]. Fortunately, it appeared that the mentioned effect is of minor importance for the observed radiation, even for a rather broad range variation of the destruction coefficient. It is shown [3] that the averaged characteristics of the line radiation emerging from a multicomponent stochastic atmosphere computed for Non-LTE lines only quantitatively differ from those for LTE lines. This requires a comprehensive study of the LTE lines as a convenient and instructive case in revealing the specificity of the line radiation emitting by a multicomponent stochastic atmosphere with allowance for the velocity field. The mean statistical quantities derived theoretically for this radiation are compared with those obtained from observations, thus providing additional information on the geometrical and physical parameters of prominences. From this point of view, the high-resolution observational data available nowadays, thanks to the SOHO space mission, afford an opportunity for applying the statistical approach in different frequencies within a line. The SUMER spectrometer slit with a $1'' \times 120''$ field makes it possible to obtain a fairly large number of profiles of different spectral lines in the EUV domain (including lines of the Lyman series) and to trace their variation along the slit. This obviously provides more information for investigation than former observations by the HCO spectrometer aboard the ATM-Skylab, which dealt merely with the integrated intensities of spectral lines. The purpose of this paper is twofold. On the one hand, we intend to collect all the results obtained in the above-cited papers for the LTE lines formed in a static atmosphere. However, more attention now will be paid to the dependence of these results on the number of structural elements. On the other hand, we extend the theory previously developed for the LTE atmosphere to allow for the velocity field. The effects of the large-scale motions, as well as micro turbulence, are envisaged. The SOHO/SUMER observational data concerning the mean profile and proper RelMSD for a number of the strongest EUV-lines of prominence are presented in the final section.

STATEMENT OF THE PROBLEM; BASIC EQUATIONS

One of the advantages of the SOHO/SUMER project is the appeared opportunity to study the EUV line profiles, which allow posing and solving more realistic frequency-dependent models in theoretical interpretation. Another advantage concerns the high resolution. The $1'' \times 1''$ observing aperture of the spectrometer implies that each pixel encompasses most probably only one row of threads along the line of sight (we take the usually accepted estimates for dimensions of the prominence threads [6]). Therefore, the consideration of the slab model may be regarded as justified, even for prominences having a vertical palisade-like structure. Finding the line intensity for given pixels reduced to a solution of a well-defined deterministic problem. Having a sufficiently large sample of data, one may find an averaged value of the line intensity and its variance in diverse frequencies. We start by presenting the law of addition of layers for the LTE atmosphere, i.e. when there is no scattering process in the medium. Let us consider two self-radiating layers, each of the optical thickness τ_1 and τ_2, and also the intensity $I(\tau_1 + \tau_2)$ of radiation escaping from the boundary $\tau_1 + \tau_2$ of the composite medium. Then, simple reasoning for the scalar case yields:

$$I(\tau_1 + \tau_2) = I(\tau_1)\exp(-\tau_2) + I(\tau_2), \tag{1}$$

where $I(\tau_1)$ and $I(\tau_2)$ are intensities of radiation emitted by each of two layers to the observer. Since the different frequencies (directions) are not coupled in the absence of scattering, generalization of Equation 1 to the non-scalar case of the line radiation is straightforward:

$$I(\tau_1 + \tau_2, z) = I(\tau_1, z)\exp(-z\tau_2) + I(\tau_2, z), \tag{2}$$

where, for brevity, we designate by z the combination $z = v(x)/\eta$ and introduce the following notations: $v(x) = \alpha(x) + \beta$, $\alpha(x)$ is the non-normalized profile of the absorption coefficient, x is the dimensionless frequency denoting the displacement from the center of the line in the Doppler widths, β is the ratio of the absorption coefficient in continuum to that in the center of the line, and η is the cosine of the angle between normal to the boundary of the medium and the direction of the radiation propagation.

In writing Equations 1 and 2, no assumptions are made as to the properties of the considered media. Indeed, each of them may be inhomogeneous, multicomponent with arbitrarily complex structure and, finally, they may undergo random variations in space obeying arbitrary statistics. We are interested in the case when two media are multicomponent and stochastic and the realizations of their parameters are statistically independent. Then, it is easy to derive that:

$$< I(\tau_1 + \tau_2, z) > = < I(\tau_1, z) >< \exp(-z\tau_2) > + < I(\tau_2, z) > . \tag{3}$$

This implies that, in the absence of scattering, the averaging process may be performed in parts. In other words, the averaged characteristics of radiation emerging from a given medium are not affected as a result of the addition of new medium to them.

Let us now consider the multicomponent medium composed of $N-1$ structural elements, each of which being characterized by optical thickness, power of internal energy sources and velocity field. The statistics of random variations of the mentioned quantities may vary from one component to another. If we add to this medium a single element, on the basis of Equation 3, we may write:

$$< I_N(z) >=< I_{N-1}(z) > q^{(N)}(z) + < I_1^{(N)}(z) >, \qquad (4)$$

where, for brevity, it is denoted that $q^{(N)}(\tau, z) =< \exp(-z^{(N)}\tau^{(N)}) >$. The superscript, N, indicates the ordinal number of statistics. Successive use of Equation 4 yields:

$$< I_N(z) > = \sum_{k=1}^{N-1} < I_1^{(k)}(z) > \prod_{i=k+1}^{N} q^{(i)}(z) + < I_1^{(N)}(z) > . \qquad (5)$$

In particular cases, when random varying parameters of all components obey the same statistics, we obtain:

$$< I_N(z) >= L_N(z) < I_1(z) >, \qquad (6)$$

where:

$$L_N(z) = [1 - q^N(z)]/[1 - q(z)].$$

Equation 6 was obtained for the simplest model problem to be described later [7]. We see that the intensity of outgoing radiation is completely determined by optical and statistical properties of a single structural element. Similar reasoning allows one to find;

$$< I_N^2(z) > = M_N(z) < I_1^2(z) > + 2K(z)A_N(z) < I_1(z) >, \qquad (7)$$

where we have introduced the following notations:

$$M_N(z) = [1 - \overline{q}^N(z)]/[1 - \overline{q}(z)],$$

$$\overline{q}(z) =< \exp(-2z\tau) >,$$

$$K(z) =< I_1(z)\exp(-z\tau) >,$$

$$A_N(z) = [L_N(z) - M_N(z)]/[q(z) - \overline{q}(z)]. \qquad (8)$$

Equations 6 and 7 are used to determine the requisite averaged values of emerging intensity and RelMSD, δ, defined as:

$$\delta(z) = [< I_N^2(z) > / < I_N(z) >^2] - 1.$$

Note that, as $N \to \infty$, i.e. in the particular case of a semi-infinite multicomponent and stochastic atmosphere, Equation 6 simplifies to:

$$< I_\infty(z) >=< I_1(z) > /[1 - q(z)]. \qquad (9)$$

This equation may be derived immediately by employing Ambartsumian's invariance principle applied to the LTE atmosphere [8]. It should be noted that in conclusion, in some cases we need to account also for the random variations of the number of components. The simplicity of formulas given by Equations 6 and 7 allows one to derive analytic expressions for the mean statistical characteristics of the observed line radiation. Indeed, assuming, for instance, that random variations of N are given by the Poisson law, after some simple algebra we obtain:

$$< I_{\overline{N}}(z) >= 1 - q(z)\exp\{-\overline{N}[1 - q(z)]\}, \qquad (10)$$

and:

$$\delta_{\overline{N}}(z) = \{\overline{q}(z)\exp[-\overline{N}(1 - \overline{q}(z))] - q^2(z)\exp[-2\overline{N}(1 - q(z))]\}/ < I_{\overline{N}}(z) >^2, \qquad (11)$$

where $\overline{N}$ is the Poisson mean number of structural elements.

NUMERICAL RESULTS; STATIC CASE

In order to find out the general pattern of intensity fluctuations observed in one or another case and to look into a wide diversity of situations, we begin with a modified version of the simple discrete model problem considered recently [7]. Following them, we assume that a multicomponent atmosphere consists of two types of component, each of which is described by an optical depth, τ_i $(i = 1, 2)$, measured in the center of the line and by a power, $B_i v(x)$, of initial energy sources. Despite the relative simplicity, this model makes it possible to make an idea on the most important features of the line shapes and their fluctuations, when they are formed in a multicomponent stochastic atmosphere. On the other hand, in some cases, it is easily generalized in order to consider more complicated and realistic models. Indeed, the physical considerations and ratiocinations underlying Equations 6 and 7 do not depend on the number of the possible values taken by the pair of parameters (B, τ). Moreover, they remain true also for the cases when the mentioned parameters are continuum-valued quantities.

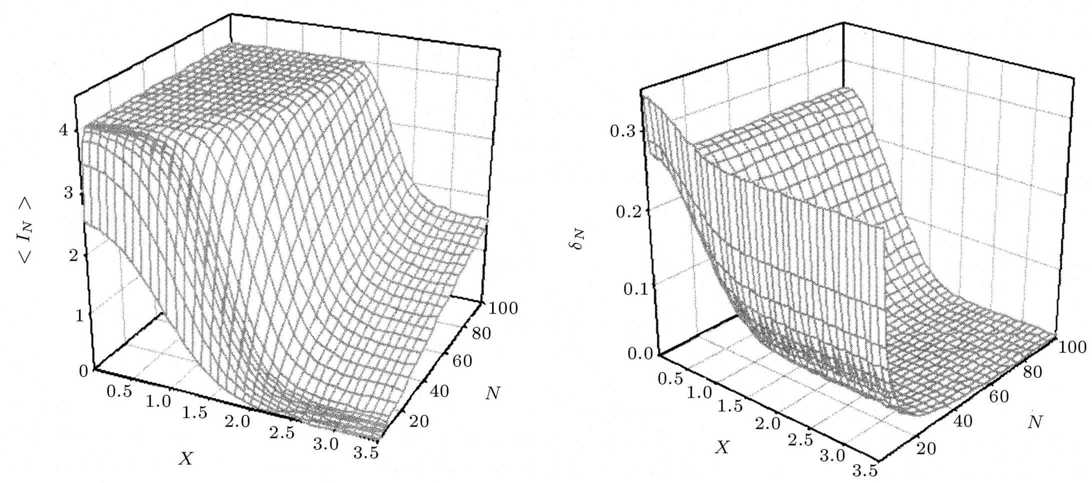

Figure 1. The intensities (left) and RelMSD (right) for radiation emerging from a multicomponent stochastic atmosphere with the Voigt function taken as the absorption coefficient profile and the following values of parameters: $B_2/B_1 = 7$, $\tau_1 = \tau_2 = 1$, $p_1 = p_2 = 0.5$, $\eta = 1$, $\beta = 10^{-2}$ and $\sigma = 10^{-2}$. The trivial case of $N = 1$ for which $\delta(x) = \text{const}$ $(= 0.44)$ is not displayed to make the right-hand side picture more visualizible.

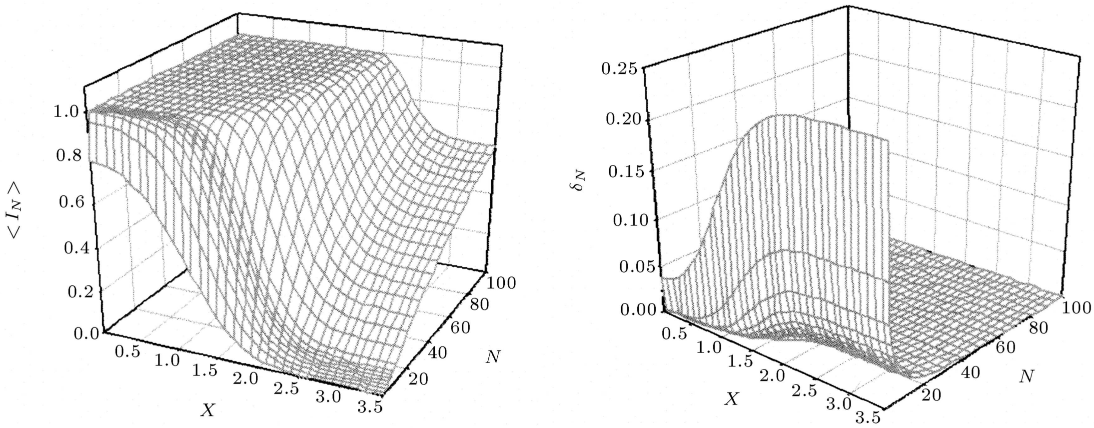

Figure 2. The same as in Figure 1 for the following values of parameters: $B_1 = B_2 = 1$, $\tau_1 = 3$, $\tau_2 = 1$, $p_1 = p_2 = 0.5$, $\eta = 1$, $\beta = 5.10^{-3}$ and $\sigma = 10^{-2}$.

The results of computations based on Equations 6 and 7 can be formulated as follows: When the fluctuations of the intensity of radiation escaping the multicomponent atmosphere are due to random variations only in the distribution of internal energy sources, the RelMSD decreases monotonically from the center of the line to its wings (typical example is displayed in Figure 1). Meanwhile, when the fluctuations are due to random changes only in the components' optical thickness, the RelMSD of the measured intensity increases from the line center to its wings (Figure 2). This effect was described for relatively small numbers of N [3]. It was also shown that inclusion of a multiple scattering process taken into consideration leads only to quantitative changes.

As shown in Figures 1 and 2, with increasing N, the length of the flat core of the line profiles becomes greater. When $N \to \infty$, the profiles in both examples disappear, tending to the constant value $\sum B_i/n$ (where n is the number of types of components) in the first case, and to $B = B_i$ in the second case.

Let us turn now to the general case when both of the two characteristics of the medium undergo random variations. To look into a huge variety of situations, due to different correlations between opacities of structural elements and the power of the energy sources they contain, one must distinguish two important types of atmosphere. It is physically reasonable to assume that the energy sources are greater in the more opaque components of the medium. We refer to this type of atmosphere as belonging to the first class. The opposite case is apparently of theoretical interest and will be considered as well. So, we call an atmosphere as second class, if the greater sources of energy are contained in the optically thinner components. These two classes of atmosphere possess quite different statistical properties. Typical examples, shown in Figures 3 and 4, demonstrate the run of the mean intensities and proper RelMSD versus frequency within the line and the number, N, of structural elements. It is seen that the RelMSD of the line-radiation outgoing from the atmosphere of the second class decreases in passing from the center of the line to its wings. This relation for the atmosphere of the first class is more complex: The RelMSD first decreases and then increases in the far wings. Nevertheless, beginning from a certain number of N, the values of RelMSD in the wings of a line are less than those in the central frequencies. It is noteworthy that, in some cases, the LTE lines may exhibit double-peaked and distorted profiles, as seen in Figures 3 and 4. All the described effects qualitatively remain in force in the case of smaller η, which is equivalent to consideration of correspondingly greater optical thicknesses for structural elements. The strong relationship between the frequency-dependent RelMSD and physical properties of the multicomponent stochastic atmosphere (at least for smaller N) allows one to have a rough idea of some characteristics of the radiating medium. Before analyzing the observed profiles and their surface variations, we note that the difference between the above-mentioned two classes of stochastic media is much more profound and goes beyond the effects described. For instance, in the limit of semi-infinite atmospheres of the first type, we observe absorption lines (Figure 5a), while the atmosphere of the second type yields an emission profile (Figure 5b). The effects of absorption in continuum and the multiple scattering in formation of Non-LTE lines are also completely different [3].

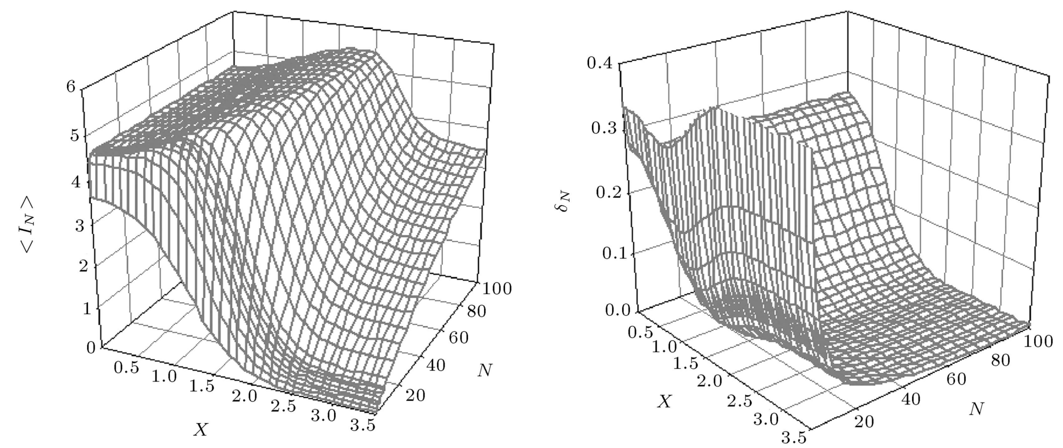

Figure 3. The mean intensities (right) and proper RelMSD (left) for radiation emerging from a multicomponent stochastic atmosphere of the first class with the Voigt function taken as the absorption coefficient profile and the following values of parameters: $B_2/B_1 = 7$, $\tau_1 = 1$, $\tau_2 = 3$, $p_1 = p_2 = 0.5$, $\eta = 1$, $\beta = 10^{-2}$ and Voigt parameter $\sigma = 10^{-2}$.

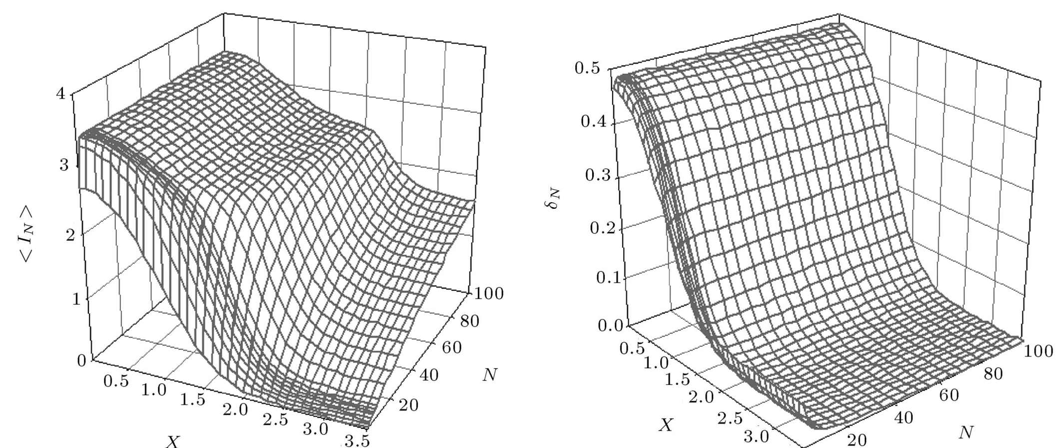

Figure 4. The same as in Figure 3 for the atmosphere of the second class and for the following values of parameters: $B_2/B_1 = 7$, $\tau_1 = 3$, $\tau_2 = 1$, $p_1 = p_2 = 0.5$, $\eta = 1$, $\beta = 10^{-2}$ and $\sigma = 10^{-2}$.

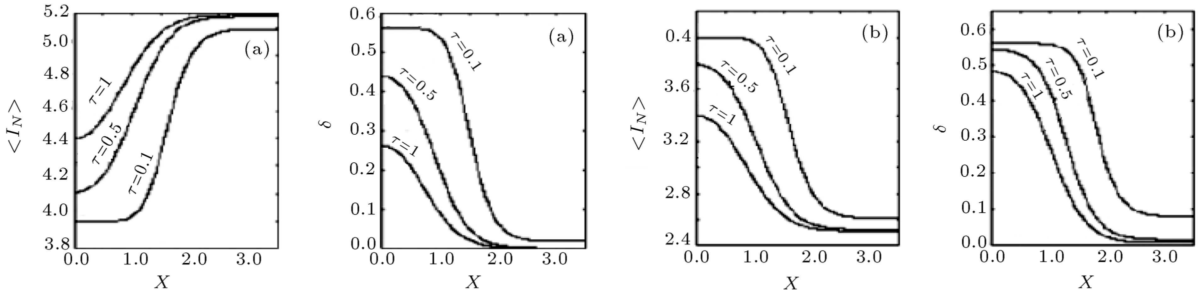

Figure 5. The profiles and RelMSD of the radiation intensity emerging from a semi-infinite multicomponent and stochastic atmosphere of the first (a) and second (b) types. The values of parameters are chosen the same as in Figures 3 and 4, respectively.

EFFECT OF THE VELOCITY FIELD

It is well established that the prominence plasma is permanently in several kinds of motion, having an influence upon the shapes of spectral lines. The random thermal and turbulent motions with $v \sim 5 \div 10$ km s^{-1} are superimposed on the ascending (eruption) or descending (mass loss to chromosphere and photosphere) large-scale bulk (or mass) motions [9]. Transfer of the line radiation through such a dynamically active multicomponent medium results in a large variety of profiles distorted, in general, due to the Doppler Effect. The net profile depends on quite a number of physical parameters describing the state of the radiating volume. We saw in the previous section that even the static atmosphere may show different profiles, depending on the slope angle of prominence with respect to the line of sight. The complex dynamic pattern leads to that one and the same spectral line may exhibit diverse profiles in different prominences or in various parts of the same prominence [10]. The variety of possible realizations makes it difficult to give a unique description of the physical properties of a radiating medium. Nevertheless, one may attempt to find out some salient features of the LTE lines originated in a multicomponent stochastic atmosphere with allowance for the turbulent and the large-scale motions.

Hydrodynamic Velocities

Large-scale motions give rise to a Doppler shift proportional to projection of the hydrodynamic gross velocity onto the line of sight, $u^{(h)}$. One may notice that the model problem considered above can be easily extended to take into consideration the velocity fields. Indeed, let us confine ourselves to considering again the transfer of radiation through a multicomponent medium consisting of discrete number n kinds of species, each of which is described now with an additional (along with the optical thickness and the power of the energy sources) parameter, $u_i^{(h)} (i = 1, 2 \cdots m)$. It is reasonable to assume that there is no correlation between the realized values of velocity and two other physical characteristics of the structural element. One may see that Equations 6 and 7 remain still in force with the only difference being that now the mean statistical quantities are supposed to include an additional averaging over possible values of hydrodynamic velocities as well. For instance, the mean opacity, q, is defined as:

$$q(x, \eta) = \sum_{i=1}^{m} \overline{p}_i \sum_{k=1}^{n} p_k \exp[-(H(x + \varpi_i, \sigma) + \beta)\tau_k/\eta], \tag{12}$$

where H is the Voigt function, $\varpi_i = u_i^{(h)}/u_{th} = (\nu_0/c)u_i^{(h)}/\Delta\nu_D$, ν_0 and $\Delta\nu_D$ are the central frequency and Doppler width of the line, c is the speed of light and $\overline{p}_i$ is the probability of occurrence of velocity $u_i^{(h)}$ for a certain component. The other mean statistical quantities undergo similar modifications. Figure 6 demonstrates a representative example of calculated profiles and proper RelMSD. As should be expected, the effect of non-thermal motions depends essentially on the value of ϖ_i and probabilities of their realization. The simple example of Figure 6 shows the blue-shifted rather distorted profiles of spectral lines. With an increase of the number of structural elements, the lines exhibit multiple-peaked (in this particular case triple-peaked) profiles. The well pronounced maximum of the RelMSD from the line center to the red-wing (i.e. in a direction opposite to the shift) for relatively small numbers on N is of interest. This feature is common for all the Doppler-shifted lines independent of the physical characteristics of components and is undoubtedly important from the diagnostic point of view.

Effect of Microturbulence

Equations derived in this paper allow one to estimate the contribution of microturbulent motion to the spectral line broadening. A simple reasoning shows that the commonly accepted way of determining the

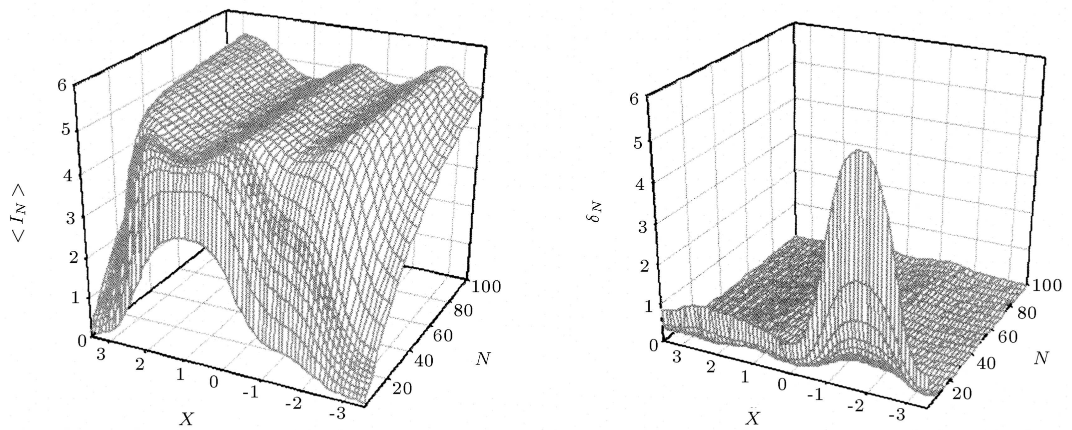

Figure 6. The observed profiles and proper RelMSD for multicomponent atmosphere considered in Figure 3, structural elements of which move with random non-thermal velocities $\varpi_1 = -1$, $\varpi_2 = 1$ occurred with probabilities $\bar{p}_1 = 0.2$ and $\bar{p}_2 = 0.8$.

microturbulence velocity, u_t, is not self-consistent and may lead to significant errors. Actually, this method is based on the identifications of the observed half width of the line with that of the profile of absorption coefficient [9,11]. It is obvious, however, that in contrast to the absorption coefficient, the line width is a physical parameter dependent on the mechanism of the line formation, optical thickness, structural pattern of radiating medium and so on. Besides, it is reasonable to regard the microturbulence as a mass motion with an infinitesimal eddy size rather than motions on the atomic level similar to thermal motions.

Let us consider this point in more detail. We shall deal with a LTE line formed in a multicomponent atmosphere of optical thickness, τ_0, in which energy sources are distributed according to the law $Bv(x)$, where B = const. For simplicity's sake, we suppose that the absorption coefficient profile is Dopplerian. We also assume that a fully developed homogeneous turbulent flow was established in the medium. Then, the probability density of the turbulent velocity, u, is given by Gaussian (see, e.g. [12,13]):

$$P(u) = \frac{1}{\sqrt{\pi} u_t} \exp(-u^2/u_t^2), \tag{13}$$

so that the mean opacity of the component of optical thickness, τ, will be given by:

$$q_a(\tau, x, \eta) = \int_{-\infty}^{\infty} P(u) \exp[-v(x - au)\tau/\eta], \tag{14}$$

where $a = u_t/u_D$. Subscript a is introduced to indicate that averaging is performed over the turbulent velocity field. Let us turn now to Equation 3 and adapt it to the problem at hand. Toward this end, we replace τ_1 by τ_0 and τ_2 by infinitesimal thickness $\Delta\tau$. Then, we may write:

$$< I(\tau_0 + \Delta\tau, x, \eta) > - < I(\tau_0, x, \eta) >= - [< I(\tau_0, x, \eta) > -B][1 - q_a(\Delta\tau, x, \eta)]. \tag{15}$$

Passing to the limit, when $\Delta\tau \to 0$, we arrive at the following differential equation:

$$\frac{d < I(\tau_0, x, \eta) >}{d\tau_0} = -\gamma(x, \eta)[< I(\tau_0, x, \eta) > -B], \tag{16}$$

where:

$$\gamma(x, \eta) = \lim_{\Delta\tau \to 0} \frac{1 - q_a(\Delta\tau, x, \eta)}{\Delta\tau}. \tag{17}$$

The solution of Equation 16 is:

$$< I(\tau_0, x, \eta) >= B[1 - e^{-\gamma(x,\eta)\tau_0}]. \tag{18}$$

One may use Equations 17 and 14 to derive an analytical expression for function γ:

$$\gamma(x, \eta) = \frac{1}{\eta} \left[\beta + \frac{\exp\left(-\frac{x^2}{a^2+1}\right)}{\sqrt{a^2 + 1}} \right]. \tag{19}$$

We see that Equation 18, for the mean observed intensity of the line, is reminiscent of the well-known classical expression for homogeneous and isothermal atmospheres given by:

$$I(\tau_0, x, \eta) = B[1 - e^{-v(x)\tau_0/\eta}]. \tag{20}$$

The only difference is that $\gamma(x, \eta)$ stands for $v(x)/\eta$, or, in other words, the contribution of the turbulent velocity field consists in replacing $\alpha(x) = \exp(-x^2)$ by $\exp\left(-\frac{x^2}{a^2+1}\right)/\sqrt{a^2 + 1}$. As $\tau_0 \to \infty$, the intensities resulting from Equations 18 and 20 tend to the same limit, B.

Now, one may imagine three ways of finding the microturbulent velocity. As mentioned above, the commonly used approach considers the influence of turbulent motions on the absorption coefficient profile, similar to that of thermal motion. In addition, the observed half-width of the spectral line is set equal to that of the absorption coefficient profile, which approximately stands for small optical thicknesses and $\beta = 0$, $\eta = 1$. In doing so, we ignore the physics of the problem. The requisite halfwidth is given by:

$$x_{1/2} = \Delta\nu_{1/2}/\Delta\nu_D = [(a^2+1)\ln 2]^{1/2}. \tag{21}$$

Another more correct way consists in using Equation 20, which yields:

$$x_{1/2} = [-(a^2+1)\ln(\chi(\tau_0) - \beta)]^{1/2}, \tag{22}$$

where:

$$\chi(\tau_0) = -\frac{1}{\tau_0}\ln\frac{1+\exp[-(1+\beta)\tau_0]}{2}. \tag{23}$$

Finally, if we consider the microturbulence as a small scale mass motion (i.e. not in the atomic level) with Gaussian distribution of velocities, from Equation 18, we obtain:

$$x_{1/2} = \{-(a^2+1)\ln[(a^2+1)^{1/2}(\overline{\chi}(\tau_0) - \beta)]\}^{1/2}, \tag{24}$$

where:

$$\overline{\chi}(\tau_0) = -\frac{1}{\tau_0}\ln\frac{1+\exp[-(a^2+1)^{-1/2} - \beta]}{2}. \tag{25}$$

The comparative analysis of the results obtained by these three ways is illustrated in Figure 7. It is seen that the greater the optical thickness of the radiating medium, the bigger the discrepancy of the classical result with the exact one. The latter occupies some intermediate position between results obtained through use of Equations 21 and 18. As should be expected, the more the deviations from the exact solution are pronounced, the greater the role of turbulence. In extreme cases of strongly developed turbulence, the values of the turbulent velocity estimated by the standard technique may differ from the real value several times.

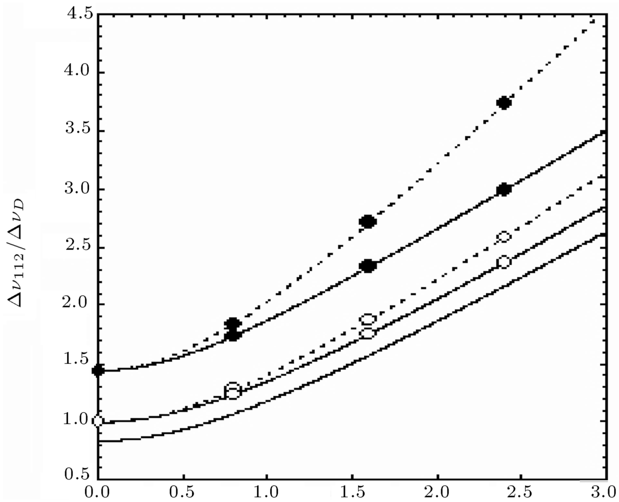

Figure 7. The halfwidths of a spectral line calculated in three different ways. Solid line: The classical result given by Equation 21; The cycled solid lines: The exact result obtained through use of Equation 24 for $\tau_0 = 1$ (open cycles) and $\tau_0 = 5$ (solid cycles). The cycled dotted lines: The results given by Equation 22 for $\tau_0 = 1$ (open cycles) and $\tau_0 = 5$ (solid cycles).

OBSERVATIONAL DATA AND DISCUSSION

SUMER is a high-resolution normal incidence spectrograph operating in the range 780-1610 Å (first order) and 390-805 Å (second order). The spatial resolution along the slit is 1 arcsec. The spectral resolution depends slightly on the wavelength. It can vary from about 45 mÅ pixel^{-1} at 800 Å to about 41 mÅ pixel^{-1} at 1600 Å [14]. A prominence situated at the limb in the south east quadrant was observed with SUMER on 8 October 1999. The pointing coordinates were $X = 362.69$, $Y = -879.75$ arcsec. The objective of this study was to make a more or less rough impression of the specificity of the line radiation in an atmosphere with a complex multicomponent structure. The spatial variations of the prominence surface brightness may often be regarded as effects concerned with random realizations of the fine structure along the line of sight. This suggests the use of a statistical approach to the problem, based on a well-developed theory. In spite of a wide variety of realizing properties of the radiating medium and different factors influencing the shape of the observed line, there exist some relationships in the measured intensities and proper RelMSD, which may be useful from a diagnostic point of view. Nevertheless, it sounds less reasonable to carry out a detailed comparison of the observational data at this stage at least for two reasons. Firstly, the specific problems treated by no means comprise all the possible variations which may be encountered; secondly, the volume of samples provided by SOHO observations is, unfortunately, not always sufficient to arrive at a unique conclusion. However, it is noteworthy to present here some results on the mean statistical characteristics of the line radiation calculated on the basis of SUMER measurements in October 1999. Figure 8 demonstrates the functional behavior of these quantities for some relatively strong EUV lines. Since the measurement errors grow to the

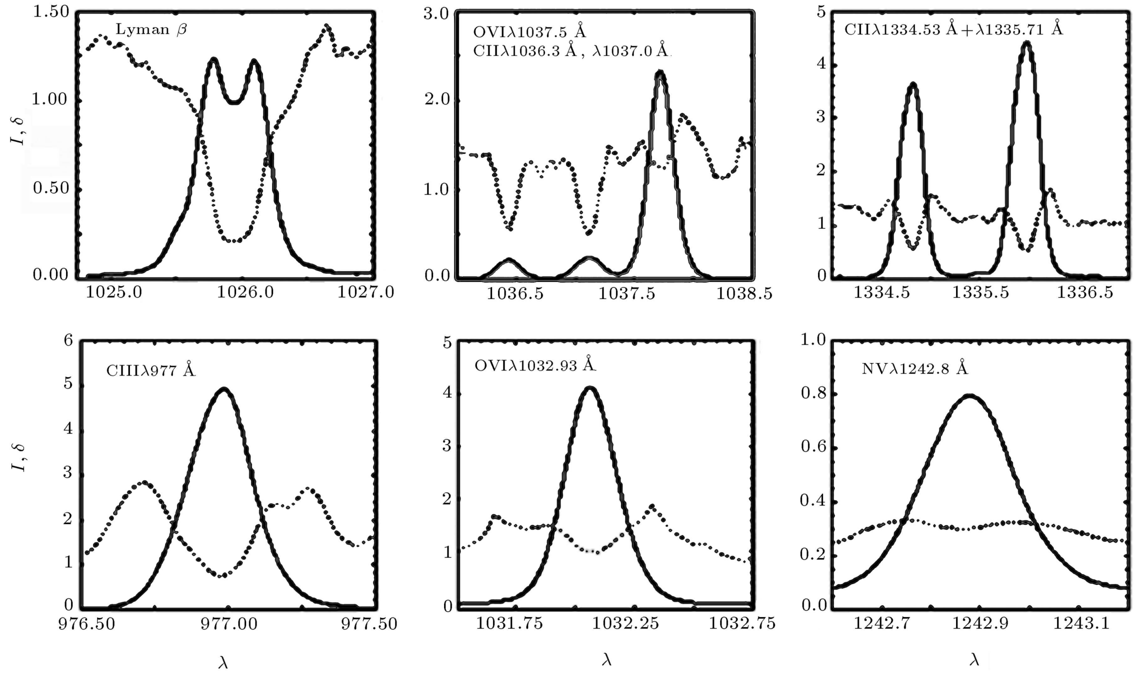

Figure 8. The profiles and the frequency dependence of RelMSD for some EUV emission lines. The numbers on the ordinate axis concern the values of RelMSD.

wings of lines, we limit ourselves to considering the frequencies not very far from the lines' center. Bearing this in mind, we see that the values of RelMSD grow in passing from the core of the line to its wings (as inferred on the basis of the theoretical investigation). The main reason for the behavior of the RelMSD is the optical depth. In the Lyman line, the line core is very opaque and we see only one element. Thus, the RelMSD is small in the line center. In the wings, we see more and more elements along the line of sight and, thus, various realizations (the number of elements) give rise to larger RelMSD. Note that such RelMSD between 1.0 and 1.5 is also detected for hotter lines, which are optically thin along the line of sight in both the line center and wings and, thus, RelMSD is constant. However, this increase is pronounced differently for various lines. For instance, among other lines, this is less noticeable for the coronal line OVI 1032 Å to have the highest effective temperature of formation. This equally concerns the other lines of this ion, particularly the line 1037 Å shown in Figure 8. Thus, we may infer that the highly-ionized plasma of this temperature is less given to variations of optical thickness. The line CIII 977 Å occupies a somewhat intermediate position in the sense that the increase to line wings is more pronounced. In general, one may notice the tendency of correlation between the depth of a central depression in RelMSD and the effective temperature of the line formation. This effect is suggested to be checked in further observations. The existence of such correlation means that the relatively cold layers of quiescent prominences are more susceptible to variations in the optical thickness. This fact is physically intelligible, because the lines with high temperature of formation are originated in the rather extended layers of the transition region and corona, where the changes in optical thickness are not remarkable.

REFERENCES

1. Nikoghossian, A.G., Pojoga, S. and Mouradian, Z. "Statistical characteristics of radiation formed in atmosphere with randomly disturbed inhomogenities", *Astron. Astrophys.*, **342**, pp. 785-798 (1999).
2. Nikoghossian, A.G. and Mouradian, Z. "Profiles of the spectral lines formed in stochastic multicomponent atmosphere", *Astron. Astrophys.*, **360**, pp. 1086-1095 (2000).
3. Nikoghossian, A.G. "Intensity fluctuations of radiation escaping from a multicomponent stochastic atmosphere. I", *Astrophysics*, **45**, pp. 223-231 (2002).
4. Nikoghossian, A.G. "Radiative transfer in one-dimensional inhomogeneous atmospheres", *Astron. Astrophys.*, **422**, pp. 1059-1066 (2004).
5. Nikoghossian, A.G., Aboudarham, J. and Mouradian, Z. "Fluctuations in the intensity of radiation emerging from a multicomponent stochastic atmosphere. II", *Astrophysics*, **48**, pp. 253-261 (2005).
6. Orrall, F.Q. and Schmahl, E.J. "The H I Lyman continuum in solar prominences and its interpretation in the presence of inhomogeneities", *Astrophysical Journal*, **240**, pp. 908-922 (1980).

7. Jefferies, J.T. and Lindsey, C. "Radiative transfer in inhomogeneous atmospheres-A statistical approach", *Astrophysical Journal*, **335**, pp. 372-382 (1988).

8. Sobolev, V.V., *Treatise on Radiative Transfer*, Princeton, Van Nostrand (1963).

9. Tandberg-Hanssen, E., *The Nature of Solar Prominences*, 3th Ed., pp. 1-50, Kluver, Dordrecht (1995).

10. Heinzel, P., Schmieder, B., Vial, J.-C. and Kotrc. "SOHO/SUMER observations and analysis of the hydrogen Lyman spectrum in solar prominences", *Astron. Astrophys.*, **370**, pp. 281-297 (2001).

11. Vial, J.-C. "Solar prominence diagnostics", *IAU Coll.167, ASP Conference Series*, **150**, pp. 175-187 (1998).

12. Batchelor, G., *The Theory of Homogeneous Turbulence*, 6th Ed., pp. 40-75, University Press, Cambridge, UK (1970).

13. Auvergne, M., Frisch, H., Frisch, U., Froeschle, Ch. and Pouquet, A. "Spectral line formation in a turbulent atmosphere", *Astron. Astrophys.*, **29**, pp. 93-100 (1973).

14. Wilhelm, K., Curdt, W., Marsch, E., Schuhle, U., Lemaire, P., Gabriel, A., Vial, J.-C., Grewing, M., Huber, M.C.E., Jordan, S.D. et al. "SUMER-solar ultraviolet measurements of emitted radiation", *Solar Physics*, **162**, pp. 189-231 (1995).